Arabian Journal of Chemistry (2020) 13, 5911–5921

King Saud University

Arabian Journal of Chemistry

www.ksu.edu.sa
www.sciencedirect.com

ORIGINAL ARTICLE

Heteropoly-12-tungstophosphoric acid $H_3[PW_{12}O_{40}]$ over natural bentonite as a heterogeneous catalyst for the synthesis of 3,4-dihydropyrimidin-2-(1H)-ones

Lakha V. Chopda [a], **Pragnesh N. Dave** [b,*]

[a] *Department of Chemistry, Krantiguru Shyamji Krishna Verma Kachchh University, Bhuj, Gujarat, India, Vallabh Vidyanagar, India*
[b] *Department Of Chemistry, Sardar Patel University, Vallabh Vidyanagar, India*

Received 11 March 2020; accepted 29 April 2020
Available online 11 May 2020

KEYWORDS

Support bentonite
$H_3[PW_{12}O_{40}]$;
Catalyst dihydropyrimidone
reusability

Abstract Heteropolyacid 12-tungstophosphoric acid $H_3[PW_{12}O_{40}]$ (TPA) immobilized over natural bentonite (bent) using the impregnation method. Prepared catalyst were well characterized by XRD, FT-IR and FeSEM. The catalytic activity of three catalysts 10%, 20% and 30% TPA/bent examined for the synthesis of 3,4-dihydropyrimidin-2(1H)-ones known as Biginelli reaction. The catalyst 30% TPA/bent exhibited a high yield of the product towards the synthesis of a variety of dihydropyrimidones (DHPMs). The high yield of dihydropyrimidone (DHPM) was obtained in model reaction in ethanol, acetonitrile and solvent - free condition. The reusability test indicated that 5% of yield of product decreased after 5th cycle.

1. Introduction

The multicomponent reactions (MCRs) is the key methodology to construct valuable heterocycles in medicinal chemistry (Biggs-Houck et al., 2010; Haji, 2016). Biginelli among multicomponent reactions is the important synthetic methodology for the preparation of diversify dihydropyrimidones (DHPMs) using a different kind of Brosnted and Lewis acids (Patil et al., 2016; Syamala, 2009). Generally, these catalysts are not sustainable in nature because of their adverse property especially the corrosive nature of these catalysts which needs specific protection at industrial - scale production. Other conventional problems related to these are the separation of catalyst, contamination in product and reusability. The use of the heterogeneous system such as zeolite, mesoporous material, clay, ion exchange resin and polymer instead of the homogeneous system is more appropriate in respect of green chemistry. In recent time, much attention has been paid to develop sustainable green process utilizing heterogeneous catalyst for Biginelli reaction (Patil et al., 2019; Shumaila and Al-Thulaia, 2019). The numerous important solid catalysts such as silica;

* Corresponding author.
E-mail addresses: lakhan.chopda@gmail.com (L.V. Chopda), pragnesh7@yahoo.com (P.N. Dave).
Peer review under responsibility of King Saud University.

Production and hosting by Elsevier

https://doi.org/10.1016/j.arabjc.2020.04.034
1878-5352

polymer, resin, clay etc were extensively studied for this reaction. Due to strong acidity, redox property, low volatility, low corrosivity, low toxicity and high thermal stability, heteropolyacids (HPAs) received significant placed in organic synthesis (Azizi et al., 2006; da Silva and de Oliveira, 2018; Heravi and Faghihi, 2014; Wang and Yang, 2015; Yadav et al., 2004). HPAs are very often used as an acid catalyst and evaluated as ideal candidature which replaced mineral acids in the proton catalyzed reaction. For instance tungsten -based HPA replaced H_2SO_4 in the hydration of alkene to alcohol (Wu et al., 1996). HPAs over solid support provide more advantages in term of catalytic activity, easy of separation and reusability. HPAs supported solid catalysts have been demonstrated for different organic reaction such as esterification (Bhorodwaj et al., 2009; Bhorodwaj and Dutta, 2011; da Conceição et al., 2019; Zhang et al., 2015), dehydration (Alharbi et al., 2015; Bond et al., 2012; Ding et al., 2017; Ladera et al., 2015; Martin et al., 2012; Parghi et al., 2011), oxidation (Rožić et al., 2015, 2011; Zhou et al., 2017), isomerization (Frattini et al., 2017; Szücs-Balázs et al., 2012) etc. (Sheng et al., 2014; Wu et al., 2016; Yang et al., 2018) (see Scheme 1).

Heterogeneous catalysts were demonstrated for MCRs. Sidorenko et al reported SO_3H functionalized various heterogeneous catalysts for multicomponent Prins-Ritter reaction of (-) isopulegol. Addition of water controlled product and stereo selectivity (Sidorenko et al., 2020). Russowsky et al used hydrotalcite (Mg/Al 3:1) known as layered or lamellar double hydroxides (LDH) for synthesis of β-Aryl-γ-nitroesters in reasonable to good yield using novel multicomponent strategy (D'Oca et al., 2016). Bosica and Zammit employed CuI-Amberlyst A-21 catalyst for nitro-Mannich reaction to synthesize β-nitroamines in good to excellent yield (Bosica and Zammit, 2018). Romanelli tested Ni-LDH which showed 90% yield of 4H-pyran using benzaldehyde, ethyl acetoacetate and malononitrile at 80 °C in solvent –free conditions (Nope et al., 2020). Jonnalagadda et al reported Ag_2O/ZrO_2 for synthesis of indenopyrimidines in more than 90% in ethanol at room temperature (Bhaskaruni et al., 2018). HPAs immobilized over solid support also reported for some MCRs. Heravi et al summarized HAPs and their heterogeneous catalyst for a variety of MCRs (Heravi et al., 2013). Azarifar et al supported preyssler-type heteropolyacid over nano TiO_2 for the synthesis of chromenes and pyrazoles assisted by ultrasound (Azarifar et al., 2014). This catalyst showed moderate to high yield of chromenes and pyrazoles respectively. Sadeghzadeh immobilized ionic liquid containing $H_3[PW_{12}O_4]$ over Fe_3O_4/SiO_2/salen/Mn and catalyst produced thiazoloquinoline in excellent yield in solvent - free condition (Sadeghzadeh, 2015). Tayebee et al prepared $H_6[P_2W_{18}O_{62}]$/pyridine-Fe_3O_4 for the synthesis of 1-aminoalkyl −2-naptholes in good to excellent yield in solvent - free condition (Tayebee et al., 2014). Application of HPAs over solid support as catalyst for Biginelli reaction has been reported in the literature. Recently Neto et al reported different loading of HPW and HSiW over zeolite Y and catalyst showed an excellent yield of product in ionic liquid (Freitas et al., 2019). Other pertinent catalysts such as Fe_3O_4@SiO_2-imid-PMA, Poly(VPyPS)-PW, 10% $H_5[PV_2W_{10}O_{40}]$/AC and PTA over chromium (II) terephthalate metal - organic framework (Javidi et al., 2015; Saikia et al., 2015; Selvakumar et al., 2018; Wang et al., 2014) and other systems as reviewed by Patil et al. (Patil et al., 2019). All system has been shown good catalytic activity towards Biginelli products. A literature reveals that $H_3[PW_{12}O_{40}]$ over natural bentonite was not studied so far for this multi component reaction. Our studied on $H_4[W_{12}SiO_{40}]$/bent(bentonite) for Biginelli reaction showed that catalyst exhibited in the range of 81–92% towards synthesis of DHPMs (V Chopda and Dave, 2020). In this work, we have used $H_3[PW_{12}O_{40}]$/bent as a novel catalyst for Biginelli reaction.

2. Experimental section

2.1. Materials

Ganatra mines and mineral, Bhuj supplied bentonite clay (95% of clay was passed from 200 mesh size sieve (BSS Standard). Heteropoly acid 12-tungstophosphoric acid $H_3[PW_{12}O_{40}]$ procured from Suvidhanath laboratory, Vadodara. The required all other chemicals used in this study purchased from Sigmaldrich and SRL.

2.2. Catalyst preparation

Preparation of all three catalysts 10%, 20% and 30% carried out using the reported method (Liu et al., 2015). Required quantity of TPA (0.5, 1 and 1.5 gm) dissolved in distilled water. These solutions added to 100 mL of a suspended solution of prescribed the quantity of bentonite (5gm of bentonite) which stirred at room temperature for 26 h. The whole solution was dried at 110 °C for 26 h.

2.3. Characterization of catalyst

X-ray diffraction (XRD) technique used for the characterization of the crystal structure of materials. XRD patterns were recorded on X'Pert PRO diffractometer with a scanning rate of 0.071112^{θ}/s using Cukα radiation (λ = 1.54 A^0) at 45 kV and 40 mA. Field emission scanning electron microscope (FeSEM) images were taken by Hitachi Japan (Model No. SU8010) and Energy dispersive spectroscopy (EDS) was obtained on Bruker Germany (Model No. XFlash6130). Fourier transform infrared (FT-IR) spectra of materials were done

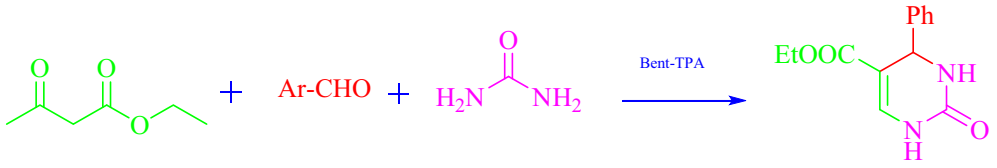

Scheme 1 Model Biginelli reaction.

in reflection mode using ZnSe optics in Bruker Alpha Eco-ATR spectrometer. The Chemical method used for element analysis. Nuclear magnetic resonance (NMR) Spectra was recorded by Brucker Advanced II 400 MHz and Brucker Advanced NEO 500 MHz spectrometer. Melting point of the compounds is recorded on SSU melting point apparatus.

2.4. General method for synthesis of DHPMs

Synthesis of DHPMs was done as per our previous reported work (V Chopda and Dave, 2020). In a particular procedure, aldehyde (2 mmol), ethylacetoacetate (2 mmol) and urea (2.4 mmol) and 0.09 gm catalyst were mixed with 20 mL of solvent in a round bottom flask. Reaction progress was monitored by thin - layer chromatography. The resulting solid materials washed with distilled water to remove unreacted urea and loaded to column chromatography (ethyl acetate /hexane mixture) for separation of product.

3. Result and discussion

3.1. Chemical and XRD analysis

The chemical analysis of bentonite is as follow: SiO_2 (54.1%), Al_2O3 (19.12%), Na_2O (0.86%), K_2O (1.32%), CaO (3.96%), FeO (3.16%), MgO (2.89%), TiO_2 (1.06%), H_2O (4.32%) and LOI (8.78). Chemical analysis shows that bentonite used in this work is Ca-bentonite (Zhirong et al., 2011). XRD analyses of all three samples are shown in Fig. 1. XRD peaks at 7.1°19.54°, 20.80°, 26.82°, 28.44°, 35.62°, 42.5° and 61.7° revealed of bentonite (Choudhury et al., 2015; Faghihian and Mohammadi, 2014; Liu et al., 2013; Yang et al., 2015). The main characteristic peak of bentonite occurred at 7.1°(d = 1.253 nm). This peak indicates of d_{001} refection of bentonite which is in accord with previously reported works (Borah et al., 2010; Liu et al., 2013; Phukan et al., 2017; Sarmah and Dutta, 2012). The intense peak at 20.80° indicates of SiO_2 crystanillity in bentonite (Wang et al., 2006). The peak at 61.7° represents of an octahedral sheet of bentonite structure (Yang et al., 2015). The XRD pattern of 10, 20 and 30% TPA/bent are pertinent to bentonite. The only difference is that all characteristic peaks of bentonite appeared at a higher angle except 19.54° and 20.80° that shifted at lower angles. The main reflection peak (d_{001}) shifted from 7.1° to 7.24° (d = 1.234 nm), 7.6° (d = 1.129 nm) and 7.96° (d = 1.112 nm) upon percentage of TPA increased. The corresponding d-spacing value was decreased. The Intensity of this peak decreased and became border with increased loading of TPA as previously reported by karthikeyan and pandurangan (Karthikeyan and Pandurangan, 2009). It gives evidence of TPA supported over bentonite. This was also upheld by shifting in others two peaks of bentonite 26.82° and 35. 62° at higher angles. Zhao et al showed that TPA displayed characteristic peaks at 2Θ = 10.°, 25.4° and 34.6° (Zhao et al., 2015). In our case, peak at 2Θ = 10.2° is not seen while reaming two peaks could be coincided with bentonite peaks due to close similarity in spectra. However, Wei et al correlate two little reflection peaks at 2Θ = 29.6° and 29.9° to $H_3[PW_{12}O_{40}]$ in HPW-Fe-Bent catalyst for degradation of methyl orange (Wei et al., 2012). These peaks are also not has been displayed by any of three XRD spectra. But two additional peaks at 27.18° and 27.43° are appeared in 10%TPA/bent which can be correlated to TPA in bentonite. These peaks disappeared in 20 & 30% TPA/bent. It shows that higher loading make homogeneous distribution of TPA over bentonite. No separate phase of TPA especially in higher loading (20 & 30% TPA/bent) was detected signifies about TPA is well disperse over bentonite, similar to that of reported by Xia et al. (Liu et al., 2015). It can be observed that drastically decline in the intensity of peak at 2Θ = 20.80° which confirmed about lost of crystanillity of SiO_2 occurred in bentonite after loading of TPA (Borah et al., 2010; Phukan et al., 2017). Further peak at 2Θ = 61.7° in all 10, 20 and 30% TPA/bent are vanished. It shows that loading leads some deformation in the octahedral sheet also.

3.2. FT-IR spectra

FT-IR spectra of raw bentonite and 10%, 20% and 30% TPA over bentonite are shown in Fig. 2. A strong band at

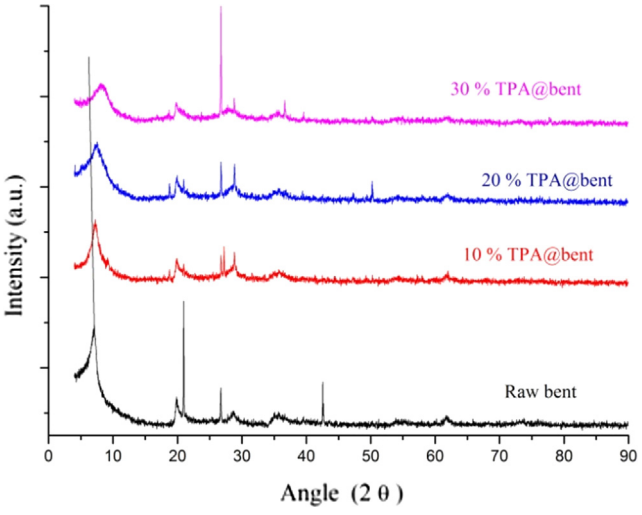

Fig. 1 XRD pattern of catalysts.

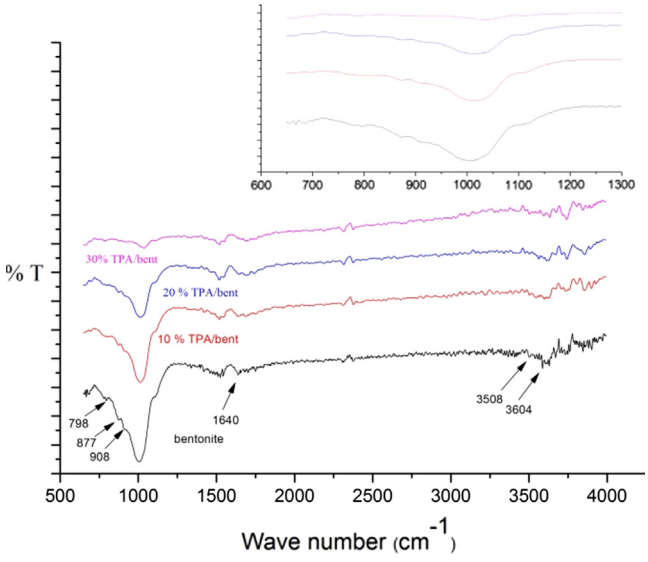

Fig. 2 FT-IR of catalysts.

1006 cm^{-1} associated to Si-O stretching vibrations (Zaitan et al., 2008). The bending vibration of Al-Al-OH appeared at 908 cm^{-1} and bands of Si-O-Al and Si-O-Si were attributed between 521 and 800 cm^{-1} (Rožić et al., 2015, 2011). The bands at 877 and 798 cm^{-1} could be associated with Si-O-Al and Si-O-Si bending vibrations respectively. The peaks appeared at 3604 cm^{-1} (Borah et al., 2010; Faghihian and Mohammadi, 2014; Liu et al., 2013; Phukan et al., 2017; Sarmah and Dutta, 2012) and 3508 cm^{-1} (Faghihian and Mohammadi, 2014) ascertained to stretching vibration of a surface hydroxyl group attached to bentonite and stretching vibration of H-O-H of adsorbed water respectively. The bands at 1640 cm^{-1} pertained to bending vibration of O-H (surface of bentonite) and H-O-H of adsorbed water (Alabarse et al., 2011; Alemdar et al., 2005; Liu et al., 2013). The FT-IR spectra of 10%, 20% and 30% TPA over bentonite have a similar pattern to raw bentonite. The only difference is that the intensity of Si-O stretching vibrations decreased at particular higher loading. The band shifted at higher wave number from 1006 to 1011 to 1016 to 1037 cm^{-1} for 10%, 20% and 30% TPA/bent respectively. It is line with XRD results in which d_{001} reflection peak shifted at a high angle as the percentage of loading enhanced from 10% to 30%. This could be revealed about the presence of TPA over bentonite. The characteristic bands of TPA such stretching band of W-O_c-W, stretching band of W-O_b-W, asymmetric W-O stretching (terminal O) and asymmetric P-O stretching were displayed at near to 804, 894, 980 and 1080 cm^{-1} respectively (Bhorodwaj and

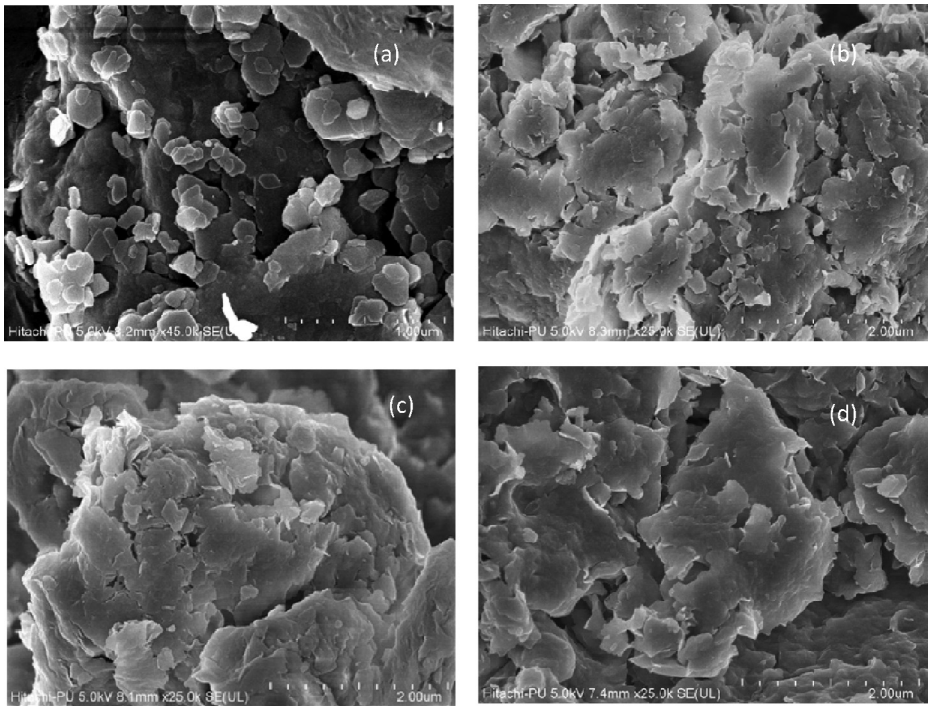

Fig. 3 FeSEM images of catalysts.

Table 1 Model Biginelli reaction.

No.	Catalyst	Solvent	Amount of catalyst (g)	Temperature (°C)	Yield
1	10% TPA/bent	Ethanol	0.09 g	80 °C	69%
2	20% TPA/bent	Ethanol	0.09 g	80 °C	81%
3	30% TPA/bent	Ethanol	0.09 g	80 °C	95%
4	30% TPA/bent	Ethanol	0.1 g	80 °C	95%
5	30% TPA/bent	Ethanol	0.15 g	80 °C	95%
6	30% TPA/bent	Ethanol	0.2 g	80 °C	83%
7	30% TPA/bent	Methanol	0.09 g	60 °C	69%
8	30% TPA/bent	Acetonitrile	0.09 g	80 °C	91%
9	30% TPA/bent	DMF	0.09 g	90 °C	82%
10	30% TPA/bent	water	0.09 g	90 °C	13%
11	30% TPA/bent	Solvent- free	0.09 g	80 °C	91%

M.P. : 205–207 (Found :206–206)[36]

[a]Reaction conditions: Benzaldehyde (2 mmol), ethylacetoacetate (2 mmol), urea (2.4 mmol), ethanol (25 mL), temperature 80 °C and reaction time 5 h.

[b]Yields refer to the isolated product.

Dutta, 2011, 2011; Karthikeyan and Pandurangan, 2009; Liu et al., 2015; Rožić et al., 2015, 2011; Wei et al., 2012; Wu et al., 2016). They are not clearly seen in 10%, 20% and 30% TPA/bent. They could be merged with bentonite peaks or not detected. It indicates that TPA homogeneously dispersed over bentonite.

3.3. Fe-SEM and EDS analysis

Fe-SEM images of raw bentonite and 10%, 20% and 30% of TPA over bentonite are shown in Fig. 3a-3d respectively. Fig. 3a (raw bentonite) shows a hexagon shape of bentonite with average particle size near 200 nm. Micrographs of Fe-SEM of TPA/Bent (Fig. 3b to 3d) are shown. The hexagon shape of raw bentonite has been visualized. It indicated that TPA is homogeneously distributed over the surface of bentonite. It is also supported by EDS analysis (shown in Fig. S1 a-d). Tungston (W) and phosphorous (P) were detected in the impregnated materials. The detailed analysis of EDS of all four catalysts is shown in Table S1. The EDS results also provided evidence of anchoring of TPA in bentonite.

3.4. Catalytic activity

The catalytic activity of 10%, 20% and 30% TPA /bent catalysts was investigated for the synthesis of versatile dihydropyrimidones known as Biginelli reaction. For this, the reaction between benzaldehyde, ethylacetoacetate and urea was selected as a model reaction in the presence of 0.09 gm of 10%, 20% and 30% TPA/bent catalysts in ethanol at 80 °C and 2:2:2.4(mmol) reactants ratio of benzaldehyde, ethylacetoacetate and urea as optimized in our reported work (V Chopda and Dave, 2020). Initially, reaction was performed in ethanol because this reaction reported in ethanol (Gangadasu et al., n.d.; Ghorbani-Choghamarani and Zamani, 2013; Jetti et al., 2012; Lima et al., 2014; Lin et al., 2007; Pansuriya et al., 2009; Phukan et al., 2017; Qiu et al., 2014; Sharghi and Jokar, 2009) and most of literature reported that high yield of product obtained in ethanol. Table 1 illustrates that catalysts 10%, 20% and 30% TPA/bent exhibited 69%, 81% and 95% yield of product of concern dihydropyrimidone (entry 1 to 3). The higher percentage of W present in 30% TPA/bent caused a high yield the of product than 10% and 20% of TPA/bent. The effect of amount of catalyst over the yield of product was conducted in ethanol at 80 °C. The effect of loading of 30% TPA/bent showed that when the amount of catalyst enhanced from 0.09 gm to 0.1 to 0.15 gm, there is no change in yield of the product (entry no. 4 & 5) but the yield of product decreased from 95% to 83% at 0.2 g of catalyst (entry no. 5). After obtained best result with 0.09 g of 30% TPA/bent, model reaction performed in different solvents. It is evident that solvents played significant role in the yield of product (Kalbasi et al., 2012; Kolvari et al., n.d.; Zolfagharinia et al., 2017). The result of this reaction was shown in Table 1 (entry 7 to 11). It shows that 91% and 82% yield of product was gained in acetonitrile and DMF respectively. However, 69% yield was achieved in methanol. When reaction carried out in solvent - free condition, 91% yield of product achieved at 80 °C which was higher than DMF and same activity as obtained in acetonitrile.

Table 2 Synthesis of dihydropyrimidones.

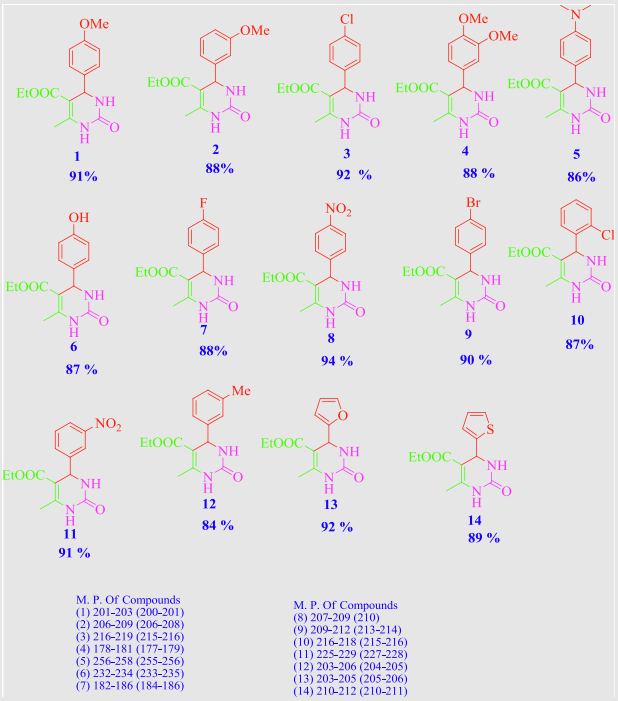

Ref. [1,3,8,9,10,11,13 & 14 (Javidi et al., 2015), 4 &6 (Kolvari et al., 2016), 5 (Wu et al., 2020), 2 &7 (Dhumaskar et al., 2014) and 12 (Debache et al., 2006)].

[a]Reaction conditions: Aldehydes (2 mmol), ethylacetoacetate (2 mmol), urea (2.4 mmol), ethanol (25 mL), temperature 80 °C and reaction time 5 h.

[b]Yields refer to the isolated product.

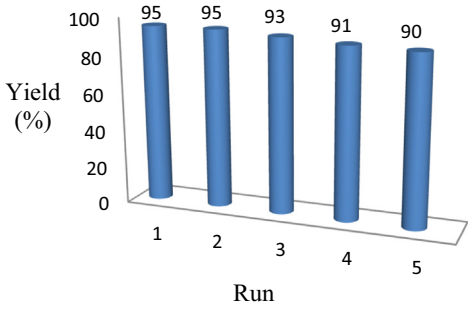

Fig. 4 Reusability of 30% TPA/bent.

The effect of raw bentonite was also checked out in our previous work (V Chopda and Dave, 2020). The raw bentonite produced 20% yield of product at 80 °C in ethanol after 48 h and 0.09 gm of amount of catalyst. At optimized conditions (0.09 gm of catalyst in ethanol at 80 °C) used for the preparation of variety of DHPMs by using 30% TPA/bent. Aromatic aldeyhydes possessing electron - donating and withdrawing groups were reacted with ethyl acetoacetate and urea that yielded more than 80% yield of relating DHPMs. The two heterocyclic compounds such as thiophen-2- carbaldehyde and

furan-2-carbaldehyde (entry 13 & 14, Table 2) were also well reacted with ethyl acetoacetate and urea to produce respective DHPMs in a good amount of yield. In compare to our reported work of $H_4[W_{12}SiO_{40}]$/bent (V Chopda and Dave, 2020), $H_3[PW_{12}O_{40}]$/bent displayed a high activity.

The reusability test of 30% TPA/bent was studied to check its efficiency under optimized conditions. The model reaction was done in five cycles. The results of reaction are shown in Fig. 4.The yield of product was 95%, 95% 93%, 91%, and 90% after 1st, 2nd, 3rd, 4th and 5th round. It directs that 5% efficiency of the catalyst was deteriorated after 5th round. However, it is not a high loss of efficiency. This could be possible that no TPA or less TPA came out (leaching out) after 5th round. The comparison of 30 %TPA/bent with other

Table 3 Comparison of catalyst.

Entry	Catalyst	Condition	Amount of catalyst	Time	Yield	Ref.
1	nano-Fe_3O_4@ZrO_2/HPW (1:2:1.5)*, [1]	100 °C(solvent free)	0.15 mmol	15 min	97%	(Zolfagharinia et al., 2017)
	Fe_3O_4@SiO_2-imid-PMA (1:1:1.5)*	80 °C(solvent free)	0.03 g	30 min	93%	(Javidi et al., 2015)
2	PTA@MIL-101(1:1:1.5)*	100 °C (solvent free)	0.6 mol%	1 h	90%	(Saikia et al., 2015)
3	28%/HSiW/Y (1:1:1)*	100 °C (BMI·PF_6)	0.051 g	1 h	99%	(Freitas et al., 2019)
4	AT-Mont (2:2:3)*	78 °C (Ethanol)	0.02 g	2 h	98%	(Phukan et al., 2017)
5	n-ZrSA (1:1:1)*	90 °C(solvent- free)	10 mol %	30 min	98%	(Kolvari et al., 2016)
6						
7	Present work (2:2:2.4)*	80 °C(ethanol and solvent-free)	0.09 g	5 h	95%, 91%	–

* Indicates mmol ratio of benzaldehyde, ethylacetoacetate and urea.
[1] Used ammonium acetate instead of urea.

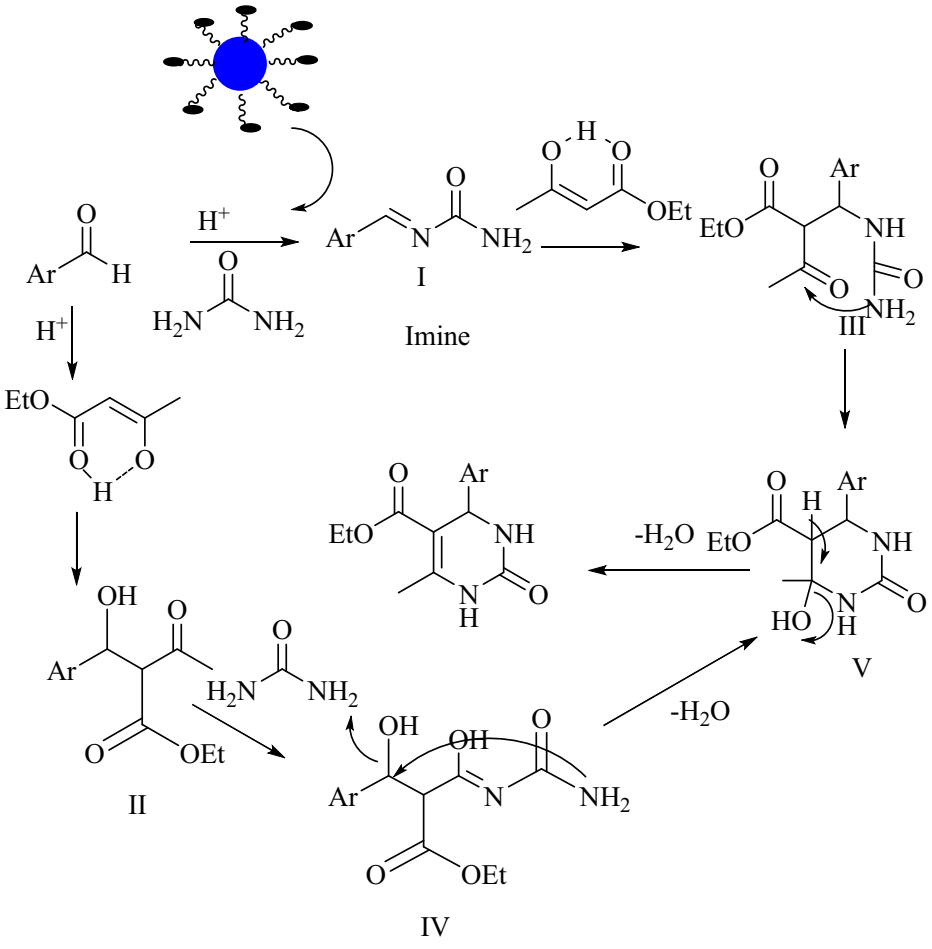

Fig. 5 Possible reaction mechanism.

closely related catalyst is shown in Table 3. Catalysts displayed in Table 3 have activity more than 90%. 30%TPA/bent also exhibits 95% and 91% in ethanol and solvent-free condition respectively.

4. Reaction mechanisms

Considering the general mechanistic pathway, the possible reaction mechanism of 30% TPA/bent catalyst displayed in Fig. 5. Protonation of carbonyl group by Bronsted acid side of catalyst produces electrophilic centre at carbony carbon. A Nucleophilic attack by urea or ethylacetoacetate happens to generate iminium (I) or Knoevenagel (II) intermediates. These intermediates could be rate - determining step in this reaction. Iminium (I) or Knoevenagel (II) intermediates react with ethylacetoacetate and urea respectively. In the case of the imine with ethyacetoacetate furnished intermediate III and Knoevenagel intermediate reacts to urea produced intermediate IV. Both intermediates underwent cyclization (intermediate V) to generate dihydropyrimidone. In a comparison of intermediates I & II, intermediate I preferred over II because of high nucleophilicity of urea than ethylacetoacetate. The third possible reaction mechanism was proposed in the literature for this reaction. It is proceeding through enamine. It occurs by nucleophilic attack of urea to ethylacetoacetate but chance of this pathway is a very negligible due to the acidic nature of catalyst.

5. Conclusions

In this work, 12-tungstophosphoric acid $H_3[PW_{12}O_{40}]$ supported over bentonite. The catalytic activity of prepared three catalysts was evaluated between benzaldehyde, ethylacetoacetate and urea as a model reaction in a different solvent. The corresponding Biginelli product was obtained in 95%, 91% and 91% in ethanol, acetonitrile and solvent - free condition. The different DHPMs were synthesized in good yield in ethanol at 80 °C. The reusability study signified that catalyst showed 90% yield of the product after the 5th cycle.

NFMR Spectral Data

5-(Ethoxycarbonyl)--6-methyl-3,4-dihydropyrimidin-2(1H) -one (Table 1, Entry no. 3).

^{1}HNMR (DMSO d_6) δ:**1.09** [t, 3H(–$OCH_2\underline{CH_3}$), ***J* = 7.0 Hz**],**3.98** (q,2H ($O\underline{CH_2}CH_3$), ***J* = 7.0 Hz**],**2.24** [s,3H (–CH_3)],**5.14** (s,1H (–CH)], **7.24** [m,3H (Ar-H), ***J* = 5.5 Hz**],**7.32**[m, 2H,(Ar-H), ***J* = 7.5 Hz**], **7.73**[s,1H,NH] and **9.19** [s,1H,NH]. ^{13}C NMR: δ: **14.03**, **17.75**, **53.93**, **59.15**, **99.22**, **126.21, 127.23, 128.35, 144.83**, **148.32**, **152.13** and **165.30.**

5-(Ethoxycarbonyl)-4-(4-methoxyphenyl)-6-methyl-3,4-dih ydropyrimidin-2(1H)-one (Table 2, Entry no. 1).

δ:**1.10** [t, 3H(–$OCH_2\underline{CH_3}$), ***J* = 7.0 Hz**],**3.97** (q,2H ($O\underline{CH_2}$-CH_3), ***J* = 7.0 Hz**],**2.23** [s,3H (–CH_3)], **3.71** [s,3H(OCH3)], **5.08** (s,1H (–CH)], **6.87** [m,2H (Ar-H), ***J* = 2.0 Hz**],**7.14** [m, 2H, (Ar-H), ***J* = 3.0 Hz**] ,**7.66** [s,1H,NH] and **9.15** [s,1H,NH]. ^{13}C NMR: δ: **14.05**, **17.72**, **53.31**, **54.98**, **59.11**, **99.53**, **113.14**, **127.37**, **137.01**, **147.97**, **152.17**, **158.40** and **165.34.**

5-(Ethoxycarbonyl)-4-(3-methoxyphenyl)-6-methyl-3,4-dih ydropyrimidin-2(1H)-one (Table 2, Entry no. 2).

δ:**1.11** [t, 3H(–$OCH_2\underline{CH_3}$), ***J* = 7.0 Hz**],**3.99** (q,2H ($O\underline{CH_2}$-CH_3), ***J* = 7.0 Hz**],**2.24** [s,3H (–CH_3)], **3.72** [s,3H(OCH3)], **5.12** (s,1H (–CH)], **6.80** [m,3H (Ar-H), ***J* = 15.0 Hz**],**7.24** [m, 1H, (Ar-H), ***J* = 7.5 Hz**] ,**7.73** [s,1H,NH] and **9.19** [s,1H,NH]. ^{13}C NMR: δ: **14.57**, **18.23**, **54.21**, **55.43**, **59.68**, **99.63**, **112.60**, **112.86**, **118.71**, **130.01**,**146.8**, **148.89**, **152.68**, **159.68 and 165.82.**

5-(Ethoxycarbonyl)-4-(4-chlorophenyl)-6-methyl-3,4-dihy dropyrimidin-2(1H)-one (Table 2, Entry no. 3)

^{1}HNMR (DMSO d_6) δ:**1.08** [t, 3H(–$OCH_2\underline{CH_3}$), ***J* = 7.0** Hz],:**3.98** (q,2H ($O\underline{CH_2}CH_3$) ***J* = 2.0** Hz], **2.13** [s,3H (–CH_3)], **5.14** [s,1H(–CH)], **7.15**[(m,2H(Ar-H) ***J* = 2.0** Hz], **7.26**[m,2H(Ar-H) ***J* = 2.5 Hz], 7.75** [s,1H,NH] and **9.23** [s,1H,NH]. ^{13}C NMR: δ: **14.04, 17.77, 53.45, 59.24, 98.73, 120.28, 128.52, 131.29, 144.17, 148.71, 151.9 and 165.16.**

5-(Ethoxycarbonyl)-4-(3,4-dimethoxyphenyl)-6-methyl-3,4-dihydropyrimidin-2(1H)-one (Table 2, Entry no. 4)

^{1}HNMR (DMSO d_6) δ:**1.11**[t,3H(–$OCH_2\underline{CH_3}$),***J* = 7.0 Hz**], **3.99**[q,2H ($O\underline{CH_2}CH_3$),***J* = 7.0 Hz**], **2.24**[s,3H (–CH_3)], **5.09** (s,1H(–CH)], **3.71**[s,6H(O<u>Me</u>-Ar)], **6.72**[m,1H(Ar-H), ***J* = 2.0 Hz**], **6.84**[m,1H(Ar-H), ***J* = 2.0 Hz**], **6.88**[m,1H(Ar-H),***J* = 8.5 Hz**], **7.67** [s,1H,NH] and **9.15** [s,1H,NH]. ^{13}C NMR: δ: **14.11**, **17.11**, **53.43**, **55.35**, **55.46**, **59.14**, **99.33**, **110.40**, **111.66, 117.85**, **137.30**, **148.00**, **148.11**, **148.42**, **152.24** and **165.39**.

5-(Ethoxycarbonyl)-4-(N,N-dimethylaminephenyl)-6-meth yl-3,4-dihydropyrimidin-2(1H)-one (Table 2, Entry no. 5)

^{1}HNMR (DMSO d_6) δ:**1.11** [t, 3H(–$OCH_2\underline{CH_3}$), ***J* = 7.5 Hz**], δ:**3.97** [(q,2H ($O\underline{CH_2}CH_3$), ***J* = 3.0 Hz**], **2.22** [s,3H(–CH_3)], **2.84** [s,6H(-N,N-dimethyl)], **5.02** [s,1H(–CH)], **6.64** [m,2H(Ar-H), ***J* = 3.0 Hz**], **7.03** [m.2H(Ar-H), ***J* = 7.0 Hz**],], **7.58** [s,1H,NH] and **9.08** [s,1H,NH]. ^{13}C **NMR: δ: 14.60, 18.19, 18.24, 51.18**, **53.66**, **53.78**, **59.55**, **100.05**, **100.37**, **112.68**, **112.75**, **127.30, 127.35**, **132.92**, **133.12**, **148.01**, **148.37**, **150.22**, **150.23**, **152.78**, **165.95**, and **166.43**.

5-(Ethoxycarbonyl)-4-(4-hydroxyphenyl)-6-methyl-3,4-dihy dropyrimidin-2(1H)-one (Table 2, Entry no. 6).

^{1}HNMR (DMSO d_6) δ:**1.09** [t, 3H(–$OCH_2\underline{CH_3}$), *J* = **7.0** Hz], **3.97** [q,2H ($O\underline{CH_2}CH_3$), *J* = **7.0 Hz**], **2.22** [s,3H(–CH_3)], **9.11** [s,1H(O<u>H</u>–Ar)],**5.03** [s,1H(–CH)], **6.68** [m,2H(Ar-H), ***J* = 2.0 Hz**], **7.02** [m.2H(Ar-H), ***J* = 2.0 Hz**], **7.61** [s,1H,NH] and **9.34** [s,1H,NH]. ^{13}C NMR δ: **14.10**, **17.69, 53.26 59.06, 99.84**, **112.17**, **126.86**, **132.61**, **147.53**, **149.70**, **152.29** and **165.45**.

5-(Ethoxycarbonyl)-4-(4-fluorophenyl)-6-methyl-3,4-dihy dropyrimidin-2(1H)-one (Table 2, Entry no. 7).

^{1}HNMR (DMSO d_6) δ:**1.09** [t, 3H(–$OCH_2\underline{CH_3}$), ***J* = 7.00 Hz**], **3.98** [(q,2H ($O\underline{CH_2}CH_3$), ***J* = 2.5** Hz], **2.25** [s,3H(–CH_3)], **5.14** [s,1H(–CH),], **7.24** [(m,2H,Ar-H), ***J* = 3.0 Hz**], **7.39** [m,2H(Ar-H), ***J* = 2.5 Hz], 7.76** [s,1H, NH] and **9.24** [s,1H,NH]. ^{13}C NMR δ: **14.49, 18.23, 53.84, 59.67, 99.63, 115.5**, **115.64**, **128.68**, **128.75**, **141.58**, **141.60, 148.96, 152.48, 160.83, 162.76** and **165.72.**

5-(Ethoxycarbonyl)-4-(4-Nitrohenyl)-6-methyl-3, 4-dihydropyrimidin-2(1H)-one (Table 2, Entry no. 7).

^{1}HNMR (DMSO d_6) δ:**1.09** [t, 3H(–$OCH_2\underline{CH_3}$), ***J* = 7.0 Hz**], **3.99** [(q,2H ($O\underline{CH_2}CH_3$), ***J* = 7.0 Hz**], **2.27** [s,3H(–CH_3)], **5.27** [d,1H(–CH)], **7.51** [(m,2H(Ar-H)), ***J* = 8.5 Hz**], **8.22** [m,2H(Ar-H), ***J* = 9.0 Hz**], **7.89** [s,1H,

NH] and **9.36** [s,1H,NH]. ^{13}C NMR δ: **13.98, 17.82, 53.67, 59.35, 98.15, 123.77, 127.62, 146.67, 149.35, 151.75, 151.96** and **165.02.**

5-(Ethoxycarbonyl)-4-(4-bromophenyl)-6-methyl-3, 4-dihydropyrimidin-2(1H)-one (Table 2, Entry no. 9)

^{1}HNMR (DMSO d_6) δ:**1.09** [t, 3H(–OCH$_2$CH$_3$), ***J* = 7.0 Hz**], **3.98** [(q,2H (OCH$_2$CH$_3$), ***J* = 7.0** Hz], **2.24** [s,3H (–CH$_3$)], **5.12** [s,1H(–CH)], **7.18** [(m,2H(Ar-H), ***J* = 8.5 Hz**], **7.52** [m,2H(Ar-H), ***J* = 8.5 Hz**], **7.77** [s,1H, NH] and **9.25** [s,1H,NH]. ^{13}C NMR δ: **14.02, 17.77, 53.40, 59.22, 98.80, 128.15, 128.35, 128.67, 131.10, 131.76, 143.76, 148.68, 151.92 and 165.16**.

5-(Ethoxycarbonyl)-4-(2-chlorophenyl)-6-methyl-3,4-dihy dropyrimidin-2(1H)-one(Table 2, Entry no. 10)

δ:**0.99** [t, 3H(–OCH$_2$CH$_3$), ***J* = 7.5 Hz**],**3.89** (q,2H (OCH$_2$-CH$_3$), ***J* = 2.5 Hz**],**2.29** [s,3H (–CH$_3$)],**5.62** [(s,1H (–CH)], **7.26** [m,1H (Ar-H) ,***J* = 3.5 Hz**], **7.29** [m,2H (Ar-H), *J* = **1.5 Hz**], **7.40**[m, 1H,(Ar-H), ***J* = 1.0 Hz**] , **7.70**[s,1H,NH] and **9.29** [s,1H,NH].^{13}C NMR: δ:**14.36, 18.13, 18.21, 51.18, 51.88, 51.97, 59.53, 98.22, 98.37, 128.20, 128.22, 129.14, 129.25 ,129.53, 129.58, 129.82, 129.94, 132.16, 142.02, 142.19, 149.75, 149.93, 151.82, 151.91, 165.43 and 165.95.**

5-(Ethoxycarbonyl)-4-(3-Nitrohenyl)-6-methyl-3,4-dihydro pyrimidin-2(1H)-one (Table 2, Entry no. 11)

^{1}HNMR (DMSO d_6) δ:**1.10**[t, 3H(–OCH$_2$CH$_3$), ***J* = 7.0 Hz**], **4.0** (q,2H (OCH$_2$CH$_3$), ***J* = 4.0 Hz**], **2.27** [s,3H (–CH$_3$)], **5.30** [s,1H(–CH)], **7.67** [(m,1H,Ar-H), ***J* = 8.0 Hz**], **7.70** [m,1H(Ar-H), ***J* = 5.0 Hz**], **8.09** [(m,1H,Ar-H), ***J* = 2.0 Hz**], **8.14** [m,1H,(Ar-H), ***J* = 1.5 Hz**], **7.91** [s,1H, NH] and **9.38** [s,1H,NH]. ^{13}C NMR δ: **14.43, 18.29, 54.03, 59.88, 98.85, 121.48, 122.80, 130.67, 133.45, 147.44, 148.20, 149.86 , 152.29 and 165.54.**

5-(Ethoxycarbonyl)-4-(3-methylphenyl)-6-methyl-3,4-dihy dropyrimidin-2(1H)-one (Table 2, Entry no. 12)

δ:**1.10** [t, 3H(–OCH$_2$CH$_3$), ***J* = 7.0 Hz**],**3.98** [q,2H (OCH$_2$-CH$_3$), ***J* = 4.0 Hz**],**2.24** [s,3H (–CH$_3$)], **2.27** [s,3H (Ar-CH$_3$)],**5.10 [**(s,1H(–CH)], **7.03** [m,3H (Ar-H), ***J* = 8.5 Hz**] ,**7.20** [m,1H(Ar-H), ***J* = 7.5 Hz**], **7.69** [s,1H,NH] and **9.15** [s,1H,NH]. ^{13}C NMR:δ:**14.54, 18.25, 21.60, 54.43, 59.62, 99.77, 123.81, 127.33, 128.34, 128.77, 137.80 145.34, 148.68, 152.61 and 165.82.**

5-(Ethoxycarbonyl)-4-(furan-2-yl)-6-methyl-3,4-dihydropyr imidin-2(1H)-one (Table 2, Entry no. 13)

^{1}HNMR (DMSO d_6) δ:**1.13** [t,3H(–OCH$_2$CH$_3$), ***J* = 7.0 Hz**], **4.02** (q,2H (OCH$_2$CH$_3$), ***J* = 2.5 Hz**], **2.23**[s,3H (–CH$_3$)], **5.20**[s,1H(–CH)], **6.09** [(m,1H,(Ar-H), ***J* = 2.5 Hz**],**6.35** [(s,1H,(Ar-H),], **7.55** [s, 1H(Ar-H)], **7.75** [s,1H,NH] and **9.24** [s,1H,NH]. ^{13}C NMR δ: **14.57, 18.17, 48.18, 59.72, 97.27, 105.76, 110.81, 142.58, 149.77, 152.92, 156.36 and 165.5.**

5-(Ethoxycarbonyl)-4-(thiophene-2-yl)-6-methyl-3,4-dihy dropyrimidin-2(1H)-one (Table 2, Entry no. 14)

^{1}HNMR (DMSO d_6) δ:**1.16** [t, 3H(–OCH$_2$CH$_3$), ***J* = 7.0 Hz**], **4.06** [q,2H (OCH$_2$CH$_3$), ***J* = 7.0 Hz**], **2.22** [s,3H (–CH$_3$)], **5.41** [s,1H(–CH)], **6.89** [(m,1H(Ar-H), ***J* = 1.0 Hz**], **6.93** [m,1H(Ar-H), ***J* = 3.5**], **7.35** [m,1H(Ar-H), ***J* = 1.0 Hz**],**7.91** [s,1H,NH**] and 9.33** [s,1H,NH].^{13}C NMR δ:**14.59, 18.13, 18.17, 49.77, 49.83, 51.35, 59.85, 100.09, 100.32, 123.99, 124.04, 125.08, 127.14, 127.22, 149.08, 149.17, 149.22, 149.36, 152.72, 152.76, 165.51 and 165.99.**

Acknowledgements

We acknowledge Panjab University and VGEC Chandkheda for utilizing their characterization facility.

Appendix A. Supplementary material

Supplementary data to this article can be found online at https://doi.org/10.1016/j.arabjc.2020.04.034.

References

Alabarse, F.G., Conceição, R.V., Balzaretti, N.M., Schenato, F., Xavier, A.M., 2011. In-situ FTIR analyses of bentonite under high-pressure. Appl. Clay Sci. 51, 202–208. https://doi.org/10.1016/j.clay.2010.11.017.

Alemdar, A., Güngör, N., Ece, O.I., Atici, O., 2005. The rheological properties and characterization of bentonite dispersions in the presence of non-ionic polymer PEG. J. Mater. Sci. 40, 171–177. https://doi.org/10.1007/s10853-005-5703-4.

Alharbi, W., Kozhevnikova, E.F., Kozhevnikov, I.V., 2015. Dehydration of methanol to dimethyl ether over heteropoly acid catalysts: the relationship between reaction rate and catalyst acid strength. ACS Catal. 5, 7186–7193. https://doi.org/10.1021/acscatal.5b01911.

Azarifar, D., Khatami, S.-M., Nejat-Yami, R., 2014. Nano-titania-supported Preyssler-type heteropolyacid: An efficient and reusable catalyst in ultrasound-promoted synthesis of 4H-chromenes and 4H-pyrano[2,3-c]pyrazoles. J. Chem. Sci. 126, 95–101. https://doi.org/10.1007/s12039-013-0548-x.

Azizi, N., Torkiyan, L., Saidi, M.R., 2006. Highly efficient one-pot three-component mannich reaction in water catalyzed by heteropoly acids. Org. Lett. 8, 2079–2082. https://doi.org/10.1021/ol060498v.

Bhaskaruni, S., Maddila, S., van Zyl, W., Jonnalagadda, S., 2018. Ag2O on ZrO2 as a recyclable catalyst for multicomponent synthesis of indenopyrimidine derivatives. Molecules 23, 1648. https://doi.org/10.3390/molecules23071648.

Bhorodwaj, S.K., Dutta, D.K., 2011. Activated clay supported heteropoly acid catalysts for esterification of acetic acid with butanol. Appl. Clay Sci. 53, 347–352. https://doi.org/10.1016/j.clay.2011.01.019.

Bhorodwaj, S.K., Pathak, M.G., Dutta, D.K., 2009. Esterification of acetic acid with n-butanol using heteropoly acid supported modified clay catalyst. Catal. Lett. 133, 185–191. https://doi.org/10.1007/s10562-009-0129-2.

Biggs-Houck, J.E., Younai, A., Shaw, J.T., 2010. Recent advances in multicomponent reactions for diversity-oriented synthesis. Curr. Opin. Chem. Biol. 14, 371–382. https://doi.org/10.1016/j.cbpa.2010.03.003.

Bond, G.C., Frodsham, S.J., Jubb, P., Kozhevnikova, E.F., Kozhevnikov, I.V., 2012. Compensation effect in isopropanol dehydration over heteropoly acid catalysts at a gas–solid interface. J. Catal. 293, 158–164. https://doi.org/10.1016/j.jcat.2012.06.021.

Borah, B.J., Dutta, D., Dutta, D.K., 2010. Controlled nanopore formation and stabilization of gold nanocrystals in acid-activated montmorillonite. Appl. Clay Sci. 49, 317–323. https://doi.org/10.1016/j.clay.2010.06.016.

Bosica, G., Zammit, R., 2018. One-pot multicomponent nitro-Mannich reaction using a heterogeneous catalyst under solvent-free conditions. PeerJ 6,. https://doi.org/10.7717/peerj.5065 e5065.

Choudhury, P.R., Mondal, P., Majumdar, S., 2015. Synthesis of bentonite clay based hydroxyapatite nanocomposites cross-linked by glutaraldehyde and optimization by response surface methodology for lead removal from aqueous solution. RSC Adv. 5, 100838–100848. https://doi.org/10.1039/C5RA18490H.

da Conceição, L.R.V., Reis, C.E.R., de Lima, R., Cortez, D.V., de Castro, H.F., 2019. Keggin-structure heteropolyacid supported on alumina to be used in trans/esterification of high-acid feedstocks. RSC Adv. 9, 23450–23458. https://doi.org/10.1039/C9RA04300D.

da Silva, M.J., de Oliveira, C.M., 2018. Catalysis by keggin heteropolyacid salts. Curr. Catal. 7, 26–34. https://doi.org/10.2174/2211544707666171219161414.

Debache, A., Boumoud, B., Amimour, M., Belfaitah, A., Rhouati, S., Carboni, B., 2006. Phenylboronic acid as a mild and efficient catalyst for Biginelli reaction. Tetrahedron Lett. 47, 5697–5699. https://doi.org/10.1016/j.tetlet.2006.06.015.

Dhumaskar, K.L., Meena, S.N., Ghadi, S.C., Tilve, S.G., 2014. Graphite catalyzed solvent free synthesis of dihydropyrimidin-2 (1H)-ones/thiones and their antidiabetic activity. Bioorg. Med. Chem. Lett. 24, 2897–2899. https://doi.org/10.1016/j.bmcl.2014.04.099.

Ding, J., Ma, T., Yun, Z., Shao, R., 2017. Heteropolyacid (H3PW12O40) supported MCM- 41: An effective solid acid catalyst for the dehydration of glycerol to acrolein. J. Wuhan Univ. Technol.-Mater Sci Ed 32, 1511–1516. https://doi.org/10.1007/s11595-017-1776-6.

D'Oca, C.R.M., Naciuk, F.F., Silva, J.C., Guedes, E.P., Moro, C.C., D'Oca, M.G.M., Santos, L.S., Natchigall, F.M., Russowsky, D., 2016. New multicomponent reaction for the direct synthesis of β-aryl-γ-nitroesters promoted by hydrotalcite-derived mixed oxides as heterogeneous catalyst. J. Braz. Chem. Soc. https://doi.org/10.5935/0103-5053.20160175.

Faghihian, H., Mohammadi, M.H., 2014. Acid activation effect on the catalytic performance of Al-pillared bentonite in alkylation of benzene with olefins. Appl. Clay Sci. 93–94, 1–7. https://doi.org/10.1016/j.clay.2014.02.026.

Frattini, L., Isaacs, M.A., Parlett, C.M.A., Wilson, K., Kyriakou, G., Lee, A.F., 2017. Support enhanced α-pinene isomerization over HPW/SBA-15. Appl. Catal. B Environ. 200, 10–18. https://doi.org/10.1016/j.apcatb.2016.06.064.

Freitas, E.F., Souza, R.Y., Passos, S.T.A., Dias, J.A., Dias, S.C.L., Neto, B.A.D., 2019. Tuning the Biginelli reaction mechanism by the ionic liquid effect: the combined role of supported heteropoly-acid derivatives and acidic strength. RSC Adv. 9, 27125–27135. https://doi.org/10.1039/C9RA03336J.

Gangadasu, Abf., Palaniappan, S., Rao, V.J., n.d. One-Pot Synthesis of Dihydropyrimidinones Using Polyaniline–Bismoclite Complex. A Facile and Reusable Catalyst for the Biginelli Reaction 3.

Ghorbani-Choghamarani, A., Zamani, P., 2013. Three component reactions: An efficient and green synthesis of 3,4-dihydropyrimidin-2-(1H)-ones and thiones using silica gel-supported l-pyrrolidine-2-carboxylic acid-4-hydrogen sulfate. Chin. Chem. Lett. 24, 804–808. https://doi.org/10.1016/j.cclet.2013.05.033.

Haji, M., 2016. Multicomponent reactions: A simple and efficient route to heterocyclic phosphonates. Beilstein J. Org. Chem. 12, 1269–1301. https://doi.org/10.3762/bjoc.12.121.

Heravi, M.M., Vazin Fard, M., Faghihi, Z., 2013. Heteropoly acids-catalyzed organic reactions in water: doubly green reactions. Green Chem. Lett. Rev. 6, 282–300. https://doi.org/10.1080/17518253.2013.846415.

Javidi, J., Esmaeilpour, M., Dodeji, F.N., 2015. Immobilization of phosphomolybdic acid nanoparticles on imidazole functionalized Fe $_3$ O 4 @Si$_O$ 2: a novel and reusable nanocatalyst for one-pot synthesis of Biginelli-type 3,4-dihydro-pyrimidine-2-(1H)-ones/thiones under solvent-free conditions. RSC Adv. 5, 308–315. https://doi.org/10.1039/C4RA09929J.

Jetti, S.R., Verma, D., Jain, S., 2012. An efficient one-pot green protocol for the synthesis of 5-unsubstituted 3,4-dihydropyrimidin-2(1 *H*)-ones using recyclable amberlyst 15 DRY as a heterogeneous catalyst via three-component biginelli-like reaction. ISRN Org. Chem. 2012, 1–8. https://doi.org/10.5402/2012/480989.

Kalbasi, R.J., Massah, A.R., Daneshvarnejad, B., 2012. Preparation and characterization of bentonite/PS-SO3H nanocomposites as an efficient acid catalyst for the Biginelli reaction. Appl. Clay Sci. 55, 1–9. https://doi.org/10.1016/j.clay.2011.05.015.

Karthikeyan, G., Pandurangan, A., 2009. Heteropolyacid (H3PW12O40) supported MCM-41: An efficient solid acid catalyst for the green synthesis of xanthenedione derivatives. J. Mol. Catal. Chem. 311, 36–45. https://doi.org/10.1016/j.molcata.2009.06.020.

Kolvari, E., Koukabi, N., Hosseini, M.M., Vahidian, M., Ghobadi, E., n.d. Nano–ZrO2 sulfuric acid: A heterogeneous solid acid nano catalyst for Biginelli reaction under solvent free conditions. RSC Adv. 11.

Ladera, R.M., Ojeda, M., Fierro, J.L.G., Rojas, S., 2015. TiO $_2$ -supported heteropoly acid catalysts for dehydration of methanol to dimethyl ether: relevance of dispersion and support interaction. Catal. Sci. Technol. 5, 484–491. https://doi.org/10.1039/C4CY00998C.

Lima, C.G.S., Silva, S., Gonçalves, R.H., Leite, E.R., Schwab, R.S., Corrêa, A.G., Paixão, M.W., 2014. Highly efficient and magnetically recoverable niobium nanocatalyst for the multicomponent biginelli reaction. ChemCatChem 6, 3455–3463. https://doi.org/10.1002/cctc.201402689.

Lin, H.X., Zhao, Q.J., Xu, B., Wang, X.H., 2007. A green synthesis of dihydropyrimidinones by Biginelli reaction over Nafion-H catalyst. Chin. Chem. Lett. 18, 502–504. https://doi.org/10.1016/j.cclet.2007.03.022.

Liu, D., Yuan, P., Liu, H., Cai, J., Tan, D., He, H., Zhu, J., Chen, T., 2013. Quantitative characterization of the solid acidity of montmorillonite using combined FTIR and TPD based on the NH3 adsorption system. Appl. Clay Sci. 80–81, 407–412. https://doi.org/10.1016/j.clay.2013.07.006.

Liu, R., Xia, X., Niu, X., Zhang, G., Lu, Y., Jiang, R., He, S., 2015. 12-Phosphotungstic acid immobilized on activated-bentonite as an efficient heterogeneous catalyst for the hydroxyalkylation of phenol. Appl. Clay Sci. 105–106, 71–77. https://doi.org/10.1016/j.clay.2014.12.024.

Heravi, M., Faghihi, Z., 2014. Applications of heteropoly acids in multi-component reactions. J. Iran. Chem. Soc. 11, 209–224. https://doi.org/10.1007/s13738-013-0291-8.

Martin, A., Armbruster, U., Atia, H., 2012. Recent developments in dehydration of glycerol toward acrolein over heteropolyacids. Eur. J. Lipid Sci. Technol. 114, 10–23. https://doi.org/10.1002/ejlt.201100047.

Nope, E., Sathicq, Á.G., Martínez, J.J., Rojas, H.A., Luque, R., Romanelli, G.P., 2020. Ternary hydrotalcites in the multicomponent synthesis of 4H-pyrans. Catalysts 10, 70. https://doi.org/10.3390/catal10010070.

Pansuriya, A., Savant, M., Bhuva, C., Kapuriya, N., Singh, J., Naliapara, Y., 2009. Cation exchange resin (Indion 130): An efficient, environment friendly and recyclable heterogeneous catalyst for the biginelli condensation. Lett. Org. Chem. 6, 619–623. https://doi.org/10.2174/157017809790442925.

Parghi, K.D., Satam, J.R., Jayaram, R.V., 2011. Silica supported heteropolyacid catalyzed dehydration of aldoximes to nitriles and alcohols to alkenes. Green Chem. Lett. Rev. 4, 143–149. https://doi.org/10.1080/17518253.2010.523015.

Patil, R., Chavan, J., Beldar, A., n.d. Review biginelli reactions: reagent support based approaches. World J. Pharm. Pharm. Sci. 5, 14.

Patil, R.V., Chavan, J.U., Dalal, D.S., Shinde, V.S., Beldar, A.G., 2019. Biginelli reaction: polymer supported catalytic approaches. ACS Comb. Sci. 21, 105–148. https://doi.org/10.1021/acscombsci.8b00120.

Phukan, A., Borah, S.J., Bordoloi, P., Sharma, K., Borah, B.J., Sarmah, P.P., Dutta, D.K., 2017. An efficient and robust heterogeneous mesoporous montmorillonite clay catalyst for the Biginelli type reactions. Adv. Powder Technol. 28, 1585–1592. https://doi.org/10.1016/j.apt.2017.03.030.

Qiu, Y., Sun, H., Ma, Z., Xia, W., 2014. Efficient, stable, and reusable Lewis acid–surfactant-combined catalyst: One-pot Biginelli and

solvent-free esterification reactions. J. Mol. Catal. Chem. 392, 76–82. https://doi.org/10.1016/j.molcata.2014.04.031.

Rožić, L., Grbić, B., Petrović, S., Radić, N., Damjanović, L., Vuković, Z., 2015. The tungsten heteropolyacid supported on activated bentonites as catalyst for selective oxidation of 2-propanol. Mater. Chem. Phys. 167, 42–48. https://doi.org/10.1016/j.matchemphys.2015.09.040.

Rožić, L., Grbić, B., Radić, N., Petrović, S., Novaković, T., Vuković, Z., Nedić, Z., 2011. Mesoporous 12-tungstophosphoric acid/activated bentonite catalysts for oxidation of 2-propanol. Appl. Clay Sci. 53, 151–156. https://doi.org/10.1016/j.clay.2010.09.017.

Sadeghzadeh, S.M., 2015. A heteropolyacid-based ionic liquid immobilized onto Fe $_{3}$ O 4 /Si$_{O}$ 2 /salen/Mn as an environmentally friendly catalyst in a multi-component reaction. RSC Adv. 5, 17319–17324. https://doi.org/10.1039/C4RA16726K.

Saikia, M., Bhuyan, D., Saikia, L., 2015. Keggin type phosphotungstic acid encapsulated chromium (III) terephthalate metal organic framework as active catalyst for Biginelli condensation. Appl. Catal. Gen. 505, 501–506. https://doi.org/10.1016/j.apcata.2015.05.021.

Sarmah, P.P., Dutta, D.K., 2012. Chemoselective reduction of a nitro group through transfer hydrogenation catalysed by Ru0-nanoparticles stabilized on modified Montmorillonite clay. Green Chem. 14, 1086. https://doi.org/10.1039/c2gc16441h.

Selvakumar, K., Shanmugaprabha, T., Kumaresan, M., Sami, P., 2018. Heteropoly acid supported on activated natural clay-catalyzed synthesis of 3,4-dihydropyrimidinones/thiones through Biginelli reaction under solvent-free conditions. Synth. Commun. 48, 223–232. https://doi.org/10.1080/00397911.2017.1396614.

Sharghi, H., Jokar, M., 2009. Al $_{2}$ O 3 /MeS$_{O}$ 3 H: A novel and recyclable catalyst for one-pot synthesis of 3,4-dihydropyrimidinones or their sulfur derivatives in biginelli condensation. Synth. Commun. 39, 958–979. https://doi.org/10.1080/00397910802444258.

Sheng, X., Kong, J., Zhou, Y., Zhang, Y., Zhang, Z., Zhou, S., 2014. Direct synthesis, characterization and catalytic application of SBA-15 mesoporous silica with heteropolyacid incorporated into their framework. Microporous Mesoporous Mater. 187, 7–13. https://doi.org/10.1016/j.micromeso.2013.12.007.

Shumaila, A.M.A., Al-Thulaia, A.A.N., 2019. Mini-review on the synthesis of Biginelli analogs using greener heterogeneous catalysis: Recent strategies with the support or direct catalyzing of inorganic catalysts. Synth. Commun. 49, 1613–1632. https://doi.org/10.1080/00397911.2018.1536789.

Sidorenko, Alexander Yu., Li-Zhulanov, Nikolai S., Mäki-Arvela, Päivi, Sandberg, Thomas, Kravtsova, Anna V., Peixoto, Andreia F., Freire, Cristina, Volcho, Konstantin P., Salakhutdinov, Nariman F., Agabekov, Vladimir E., Murzin, Dmitry Yu., 2020. Stereoselectivity inversion by water addition in the –SO 3 H-catalyzed tandem prins-ritter reaction for synthesis of 4-amidotetrahydropyran derivatives. ChemCatChem 12 (9), 2605–2609. https://doi.org/10.1002/cctc.v12.910.1002/cctc.202000070.

Syamala, M., 2009. Recent progress in three-component reactions. An update. Org. Prep. Proced. Int. 41, 1–68. https://doi.org/10.1080/00304940802711218.

Szücs-Balázs, J.-Z., Coroş, M., Woiczechowski-Pop, A., Blănită, G., Vlassa, M., 2012. Supported H4SiW12O40 catalysts for α-pinene isomerization. Open Chem. 10. https://doi.org/10.2478/s11532-012-0039-9.

Tayebee, R., Amini, M.M., Rostamian, H., Aliakbari, A., 2014. Preparation and characterization of a novel Wells-Dawson heteropolyacid-based magnetic inorganic–organic nanohybrid catalyst H 6 P 2 W 18 O 62 /pyridino-Fe 3 O 4 for the efficient synthesis of 1-amidoalkyl-2-naphthols under solvent-free conditions. Dalton Trans. 43, 1550–1563. https://doi.org/10.1039/C3DT51594J.

V Chopda, L., Dave, P.N., 2020. 12-Tungstosilicic acid H $_{4}$ [W $_{12}$ SiO $_{40}$] over natural bentonite as a heterogeneous catalyst for the synthesis of 3,4-dihydropyrimidin-2(1H)-ones. ChemistrySelect 5, 2395–2400. https://doi.org/10.1002/slct.201904962.

Wang, J., Zong, Y., Fu, R., Niu, Y., Yue, G., Quan, Z., Wang, X., Pan, Y., 2014. Poly(4-vinylpyridine) supported acidic ionic liquid: A novel solid catalyst for the efficient synthesis of 2,3-dihydroquinazolin-4(1H)-ones under ultrasonic irradiation. Ultrason. Sonochem. 21, 29–34. https://doi.org/10.1016/j.ultsonch.2013.05.009.

Wang, L., Lu, A., Wang, C., Zheng, X., Zhao, D., Liu, R., 2006. Nano-fibriform production of silica from natural chrysotile. J. Colloid Interface Sci. 295, 436–439. https://doi.org/10.1016/j.jcis.2005.08.055.

Wang, S.-S., Yang, G.-Y., 2015. Recent advances in polyoxometalate-catalyzed reactions. Chem. Rev. 115, 4893–4962. https://doi.org/10.1021/cr500390v.

Wei, G.-T., Fan, C.-Y., Zhang, L.-Y., Ye, R.-C., Wei, T.-Y., Tong, Z.-F., 2012. Photo-Fenton degradation of methyl orange using H3PW12O40 supported Fe-bentonite catalyst. Catal. Commun. 17, 184–188. https://doi.org/10.1016/j.catcom.2011.11.003.

Wu, P., Feng, L., Liang, Y., Zhang, X., Mahmoudi, B., Kazemnejadi, M., 2020. Magnetic Fe-C-O-Mo alloy nano-rods prepared from chemical decomposition of a screw (a top-down approach): An efficient and cheap catalyst for the preparation of dihydropyridine and dihydropyrimidone derivatives. Appl. Catal. Gen. 590,. https://doi.org/10.1016/j.apcata.2019.117301 117301.

Wu, X., Liu, Y., Liu, R., Wang, L., Lu, Y., Xia, X., 2016. Hydroxyalkylation of phenol to bisphenol F over heteropolyacid catalysts: The effect of catalyst acid strength on isomer distribution and kinetics. J. Colloid Interface Sci. 481, 75–81. https://doi.org/10.1016/j.jcis.2016.07.043.

Wu, Y., Ye, X., Yang, X., Wang, X., Chu, W., Hu, Y., 1996. Heterogenization of heteropolyacids: a general discussion on the preparation of supported acid catalysts. Ind. Eng. Chem. Res. 35, 2546–2560. https://doi.org/10.1021/ie950473s.

Yadav, J.S., Reddy, B.V.S., Sridhar, P., Reddy, J.S.S., Nagaiah, K., Lingaiah, N., Saiprasad, P.S., 2004. Green protocol for the biginelli three-component reaction: Ag3PW12O40 as a novel, water-tolerant heteropolyacid for the synthesis of 3,4-dihydropyrimidinones. Eur. J. Org. Chem. 2004, 552–557. https://doi.org/10.1002/ejoc.200300559.

Yang, S., Ren, X., Zhao, G., Shi, W., Montavon, G., Grambow, B., Wang, X., 2015. Competitive sorption and selective sequence of Cu (II) and Ni(II) on montmorillonite: Batch, modeling, EPR and XAS studies. Geochim. Cosmochim. Acta 166, 129–145. https://doi.org/10.1016/j.gca.2015.06.020.

Yang, Y., Lv, G., Guo, W., Zhang, L., 2018. Synthesis of mesoporous silica-included heteropolyacids materials and the utilization for the alkylation of phenol with cyclohexene. Microporous Mesoporous Mater. 261, 214–219. https://doi.org/10.1016/j.micromeso.2017.11.018.

Zaitan, H., Bianchi, D., Achak, O., Chafik, T., 2008. A comparative study of the adsorption and desorption of o-xylene onto bentonite clay and alumina. J. Hazard. Mater. 153, 852–859. https://doi.org/10.1016/j.jhazmat.2007.09.070.

Zhang, F., Jin, Y., Shi, J., Zhong, Y., Zhu, W., El-Shall, M.S., 2015. Polyoxometalates confined in the mesoporous cages of metal–organic framework MIL-100(Fe): Efficient heterogeneous catalysts for esterification and acetalization reactions. Chem. Eng. J. 269, 236–244. https://doi.org/10.1016/j.cej.2015.01.092.

Zhao, S., Xu, G., Chang, J., Chang, C., Bai, J., Fang, S., Liu, Z., 2015. Direct production of ethyl levulinate from carbohydrates catalyzed by H-ZSM-5 supported phosphotungstic acid. BioResources 10, 2223–2234. https://doi.org/10.15376/biores.10.2.2223-2234.

Zhirong, L., Azhar Uddin, Md., Zhanxue, S., 2011. FT-IR and XRD analysis of natural Na-bentonite and Cu(II)-loaded Na-bentonite.

Spectrochim. Acta. A. Mol. Biomol. Spectrosc. 79, 1013–1016. https://doi.org/10.1016/j.saa.2011.04.013.

Zhou, L., Wang, L., Wang, H., Cao, Y., Yan, R., Zhang, S., 2017. Silica supported heteropoly catalysts for oxidation of methacrolein to methacrylic acid. J. Thermodyn. Catal. 07. https://doi.org/10.4172/2157-7544.1000176.

Zolfagharinia, S., Kolvari, E., Koukabi, N., 2017. A new type of magnetically-recoverable heteropolyacid nanocatalyst supported on zirconia-encapsulated Fe3O4 nanoparticles as a stable and strong solid acid for multicomponent reactions. Catal. Lett. 147, 1551–1566. https://doi.org/10.1007/s10562-017-2015-7.